International Journal of Nanoelectronics and Materials
IJNeaM
ISSN 198-5761 | E-ISSN 2232-1535

Integration Of Acoustophoresis and Dielectrophoresis on A Single Chip Platform: A Numerical Study

Anjam Waheed, Muhammad Ramdzan Buyong, and M. F Mohd Razip Wee*

Institute of Microengineering and Nanoelectronics Universiti Kebangsaan Malaysia UKM Bangi, Selangor, 43600 Malaysia.
**Corresponding author. Tel: +6-03-89118561; Fax: +6-03-8925043; e-mail: m.farhanulhakim@ukm.edu.my*

ABSTRACT

Passive or active manipulation forces would be needed for the microfluidic system for chemical and biological analysis in order to regulate, trap, separate, sort, and discriminate between particles and cells. The primary goals of passive manipulation are consistency and repeatability to attain high levels of control with exact trajectories. In the meantime, by introducing external forces like hydrodynamic, dielectrophoretic, magnetophoretic, acoustophoretic, and optical tweezing, the active manipulations allow to control particle displacement in a highly predictable and consistent fashion. These methods are much more promising for the development of a small and compact biomedical diagnostic rapid test. Since most biological particles are suspended in different biological fluids like blood and urine, dielectrophoresis (DEP) and acoustophoresis (ACP) have been demonstrated to be promising among these external forces because of their ability to apply forces on the particles in a liquid environment. Additionally, both techniques are fast, inexpensive to fabricate, label-free, and incredibly selective. In this study, we introduce a novel method that combines these two forces into a single chip, improving the separation process for ACP and DEP based on the intrinsic dielectric and acoustic properties of the particles, respectively. It is anticipated that this research would shed light on why particular manipulative factors predominate more or less in particular situations.

Keywords: *Acoustophoresis, Dielectrophoresis, Microfluidics*

1. INTRODUCTION

Over the recent decades, there has been substantial progress in the field of microfluidic technologies, offering a versatile toolkit for the precise manipulation of fluid specimens, particles, and suspended cells. It offers several noteworthy advantages over traditional microscale methodologies encompassing the capacity for high-throughput analysis, precise fluid control, cost-effectiveness, reduced reagent consumption, and, notably, diminished reliance on human intervention owing to its proficient automation capabilities. [1, 2]. The aim of this technology is to revolutionize the healthcare, chemical, medical and pharmaceutical industries [3].

In medical, microfluidics is regarded as a revolutionary technology due to its ability to manipulate fluids precisely, especially in clinical diagnostics. As of now, microfluidic technologies provide a variety of ways for manipulating particles based on their physical and biological characteristics like shape, size, magnetism, density, dielectric properties etc [4]. This includes transportation, separation, trapping, and enrichment, based on either passive or active forces . Passive forces rely on channel geometry or intrinsic hydrodynamic phenomena. However, the fixed geometry and constrained design of passive micro-channels limit their ability to work with a wide range of samples. On the other hand, active forces can accurately control and provide real-time adjustments. Moreover, these forces have the advantage of being quick and precise [9]. These forces rely on external fields such as electric, magnetic and acoustic fields. Among them, the manipulation of particles due to acoustic streaming called ACP and the manipulation of particles (dielectric) due to a non-uniform electric field called DEP, have gained prominence due to cheap and easy handling. ACP has many advantages like non- invasiveness, versatility, simple fabrication and easy operation. Due to its ease of use and gentle handling, it also allows the separation and trapping system to operate in a continuous mode [10]. While DEP is not only label-free, accurate, fast, and low- cost [11, 12] also it can separate bioparticles on the basis of their sizes regardless of whether the particles are alive or dead. [13, 14]. However, DEP has a very limited throughput and only uses localized separation forces near to the electrodes [15]. On the other hand, ACP is a contactless and label-free manipulation technique which is being able to exert forces in a larger area of the micro-channel while exhibiting less selectivity. Moreover, in comparison with other shear-based manipulation method, it is harmless to living cells which makes it an excellent choice for particles manipulation [16]. In addition, the most significant aspect of ACP, is its ability to propagate and penetrate within matter without adversity which is very important for biological studies and clinical therapies [17-19]

Therefore, the integration of ACP and DEP may facilitate particle manipulation operations that would be impossible for a single one to accomplish. For example, Barbaros Cetin et al, demonstrated the ACP and DEP integration in a single microfluidic device fabrication by mechanical technique in order to perform buffer exchange at polystyrene particles

separation [20]. Moreover, Haizhen Sun et al, proposed a multifunctional approach which effectively combines alternating current electrothermal (ACET) and dielectrophoresis (DEP) flow for continuous particle switching, trapping and sorting [21]. Likewise, the combination of gravitational and magnetizing force fields is carried out for naturally air convection in a cubic enclosure [22].

In present study, a numerical analysis of ACP with DEP is carried out with the help of the COMSOL Multiphysics 5.5 software. We conduct this study to comprehensively compare ACP and DEP forces, aiming to elucidate the conditions under which one force dominates over the other. In this regard, three numerical models have been proposed employing Finite Element Method (FEM) to investigate the dynamics of particles within a microchannel. These simulations encompass three distinct scenarios employed for manipulating polystyrene particles. The selection of polystyrene particles for this study is based on their spherical shape and homogeneous characteristics, which make them a suitable choice for the numerical investigation. The results of the simulation indicate how polystyrene trajectories alter as their size changes from 0.1μm until 2.0μm. For ACP, acoustic streaming overcomes acoustic radiation force for small size particles (0.1 μm) while acoustic radiation force overcomes streaming for comparatively large size particles (1.0 μm, 2.0 μm). For DEP, attraction effect is observed for frequency 0.4MHz while repulsion effect is observed for frequency 5MHz. Moreover, for the combination of ACP and DEP, the streaming effect as well as the negative dielectrophoresis effect exist at frequency 5MHz. The findings of this study contribute to understand the fundamental and the underlying physics governing the particles trajectories. Furthermore, they offer a pathway towards enhancing the optimization and precise control of microfluidic applications reliant on ACP and DEP forces. These results have the potential to serve as a foundational framework for guiding future experimental investigations and providing valuable insights for the refinement and customization of particle separation methodologies across a wide spectrum of scientific and industrial domains.

2. SIMULATION MODEL

We developed our simulation based on Finite Element Method (FEM) using COMSOL Multiphysics 5.5 by representing a two-dimensional rectangular cross section of straight microchannel to be used as model system in our numerical study. We used a simplified microfluidic channel in order to reduce the complexity of the model. Thus, we could neglect the effect of axial dynamics. The cross section is defined by width, w = 150 μm and height, h= 100μm in the vertical yz-plane. The fluid inside the model is represented by a DI water with speed of sound = 1500m/s and density= 1000kg/m^3 which is incompressible and Newtonian fluid. In order to observe the particle movement under the effect of ACP and DEP, we employed spherical polystyrene particles with diameters of 0.5, 1.0, 2.0, 3.0, or 5.0 um, respectively modeled as monodisperse and non-interacting between each other. In the case of DEP, we introduced two electrodes (width of 60um) at the bottom of the model which include the combination of electrical current and the laminar flow interfaces. These electrodes attract (0.4MHz) or repel (5MHz) particles with force as given below.

$$F_{DEP} = 2\pi\, \varepsilon o\, \varepsilon medium\, r^3 Re\, CMF \nabla E2 \quad (1)$$

Here εo is the permittivity of free space, εmedium is the permittivity of suspended medium, r is radius and E is electric field. The Clausius–Mossoti factor (CMF) is a frequency-dependent reaction that may be expressed as follows:

$$CMF = (\varepsilon^*_{particle} - \varepsilon^*_{medium}) / (\varepsilon^*_{medium} - 2\varepsilon^*_{medium}) \quad (2)$$

Where $\varepsilon^*particle = \varepsilon_{particle} - (j\sigma_{particle})/\omega$

ε^* medium $= (j\varepsilon\sigma_{medium})/\omega$

where ε*particle and $\varepsilon_{particle}$ are the complex and absolute permittivity of particles while $\sigma_{particle}$ and σ_{medium} are the conductivity of particle and medium. We simplified this model by neglecting the effect of electrode thickness. We define the electrical potential as ±1V at each electrode and it is conducted in a frequency domain (AC). The DI water is considered as non-conductive with its permittivity = 78 and conductivity=2E-4 S/m. The boundary condition is chosen to be grounded except at the electrodes. Then we changed the operating frequency of DEP from 100kHz to 5MHz by alternating polarity at the electrode allowing to regulate the particle trajectories.

Meanwhile, the model was developed to induce ACP by exploiting the resonance of piezoelectric transducer from external ultrasound actuation source. The ultrasonic piezo transducer is simplified by using the velocity boundary condition while keeping the temperature constant. We built the model to obtain a horizontal half-wave across the width of the microchannel W which could be defined by f= v/(2p) = c0/(2w) where f is the resonance frequency of the system. Next, the external acoustic source was excited with a harmonic time dependence of frequency f and the behaviour of the piezoelectric material is ignored in the simulation. We implement simply hard wall boundary conditions on our model representing glass-silicon structure. Before we could observe the particles trajectories, we must first solve the first and second order equations of the imposed ultrasound field with further simplification by assuming that all first-order fields will have a harmonic time dependence e^{2ivt} using Thermoacoustic interface. In order to solve the second order continuity and Navier Stoke equation especially in the case of Newtonian fluid like water and most other liquids, the thermal effects in the above first-order equations could be neglected by ignoring the coupling in the second-order equations between the temperature field and the mechanical variables (pressure and velocity). It allows to get some idea of distribution of the pressure field and the amplitudes from the oscillating first-order fields inside the channel at the standing half-wave resonance resulting from the actuation at the wall excited by velocity boundary condition.

Once we calculated the first- and second-order acoustic fields, we could determine the time averaged acoustic forces on a single suspended particle induced by the acoustic radiation force F_{rad} equation due to the scattering of acoustic waves on the particle and the Stokes drag force F_{drag} equation from the acoustic streaming by neglecting the gravitational effects. The time average acoustic radiation force F_{rad} on a small single spherical particle in a viscous fluid having density ρp, radius a, and compressibility Kp in a viscous fluid is given below:

$$F_{rad} = -\pi a3[2K0/3Re[f1^* \rho p^* \nabla \rho 1] - \rho 0\ Re[f2^* V1^* .\nabla v1]] \quad (3)$$

The time averaged stokes drag force F_{drag} with velocity u, radius a and streaming velocity $<v_2>$ on a spherical particle radius, is expressed as

$$F_{rad} = 6\pi\eta a(<v_2> - u) \quad (4)$$

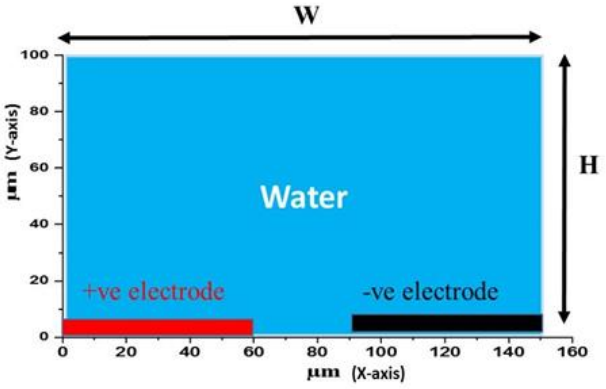

Figure 1. Cross sectional sketch of model with width w = 150μm and height h = 100μm used for simulation.

Finally, the particle tracing combined with fluid flow interface is used to compute the motion of particles in a background fluid for both ACP and DEP along with its combination. We performed the calculation of polystyrene microparticles trajectories with different radiuses (0.1μm, 0.5μm, 1.0μm and 2.0μm) suspended in water and distributed evenly with the spacing of 1.3 x 10-14/14 μm in X direction and 8.0 x 10-5/9 μm in y direction at the initial time t = 0 as shown in Figure 1.

We could obtain time-dependent motion of the particles taking into account the radiation force and the drag force for ACP while in the case of DEP, the particles movement is induced exclusively by the electric field generated at the bottom electrode and its drag force. The particles released from the grid node (its initial coordinates) at t=0 and we fixed its end after 10 s with the step of 0.5sec. Once the final position of the particles has been determined, we could indicate the instantaneous particle velocity u and the lengths of the trajectories showing the distance covered by the particles in 10 s (1).

4. RESULTS AND DISCUSSION

The results obtained from simulations for the three cases involving ACP, DEP, and their combination are found to be advantageous for the manipulation of polystyrene particles. Being homogeneous and spherical in shape, the polystyrene particles are preferred in low conductive medium like DI water. In the first case (ACP) as shown in figure 2, for radius a= 0.1μm the acoustic streaming is dominating over the acoustic radiation force and flow rolls of characteristics streaming are clearly visualized. This streaming effect is produced due to vibrating particles close to the fluid boundary in motion. Moreover, along the acoustically induced flow, the suspended particles in the fluid will rotate due to fluid drag which leads to the manipulation of particles.

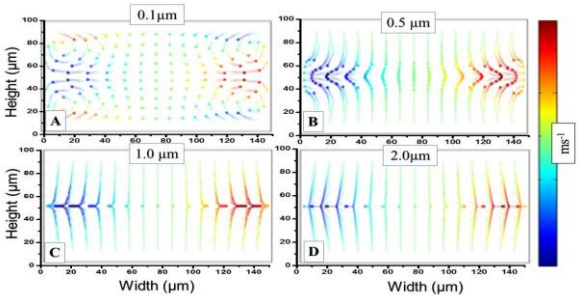

Figure 2. The trajectories (coloured part) attained via acoustophoresis at t = 5 s for four distinct particle radiuses are shown in four panels.

For the radius a=1.0μm and 2.0μm the acoustic radiation force is dominating over acoustic streaming force. In this context, the particles exhibit motion towards the horizontal pressure nodal plane. Notably, when considering particles with a radius of a=0.5μm, an intermediate regime becomes evident, wherein the combined influence of both the acoustic radiation force and the acoustic streaming force is observable. It's important to emphasize that the magnitude of this force is contingent upon the particle's radius, as well as the compressibility and density of the surrounding medium. Consequently, as particle size increases, the standing waves drive the polystyrene particles towards regions of lower pressure.

For the second case (DEP), it is seen that at particle radius a=0.1μm there is no attraction or repulsion towards or away from electrodes as shown in figure 3.

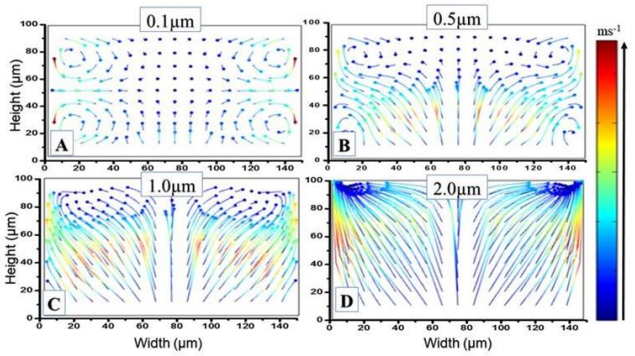

Figure 3. The trajectories (coloured lines) and places (dots) attained via electrophoresis at t = 5 s for four distinct particle diameters are shown in four panels at frequency 5.0MHz: 0.1 μm, 0.5 μm, 1.0 μm and 2.0 μm are the different sizes.

Exclusively the phenomenon of streaming is observed, attributed to the inherent challenges associated with controlling small particles, which consequently leads to a limited influence of DEP on these particles. In other cases, there is the repulsion of microparticles for radii a=0.5 μm, a=1.0 μm and a=2.0 μm. So, the particles have negative DEP if their radii are increasing. The particles with radius a=2.0 μm have more negative DEP effect as compared to particles with radii a=1.0 μm and a=0.5 μm. The reason is that, these particles (0.5 μm, 1.0 μm and 2.0 μm) are less polarizable than the surrounding medium, which makes them repel towards low electric fields.

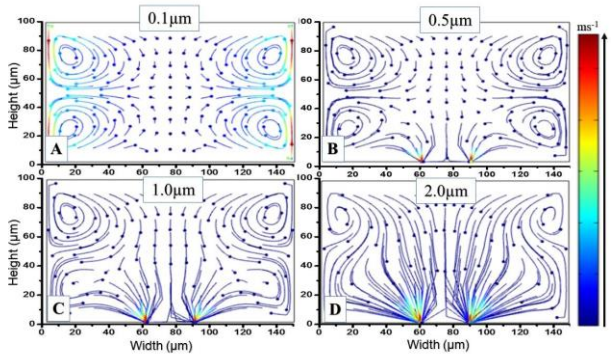

Figure 4. The trajectories (coloured lines) and places (dots) attained via electrophoresis at t = 5 s for four distinct particle diameters are shown in four panels at frequency 0.4MHz: 0.1 μm, 0.5 μm, 1.0 μm and 2.0 μm are the different sizes.

The polystyrene particles are further studied for varying radiuses (0.1 μm, 0.5 μm, 1.0 μm and 2.0 μm) at frequency f= 0.4MHz for time t=5sec as shown in figure 4. All particles' characteristics remain consistent across all figures, denoted as A, B, C, and D. In Figure 'A,' a predominant streaming effect is observable for particles with a size of 0.1 μm. As the particle size increases to 0.5 μm, Figure 'B' exhibits a minor positive dielectrophoresis effect in addition to the streaming effect. Comparatively, Figure 'C' displays a greater degree of positive dielectrophoresis than Figure 'B,' while Figure 'D' demonstrates a notably pronounced dielectrophoresis effect. The reason is that the particles are more polarizable than the surrounding medium, which makes them attract towards the electrodes. Based on these observations, it can be asserted that, at a frequency of 0.4 MHz, the electrodes exhibit an increasing attraction towards polystyrene particles with larger sizes. Additionally, it is noteworthy that the particle velocity escalates as they approach the electrodes.

In the last scenario, the combination of ACP and DEP reveals both the phenomena of particle streaming and repulsion, as illustrated in Figure 5. The four simulated figures are selected at frequency 5MHz and voltage ± 1V in which clear behaviour of particles can be visualized.

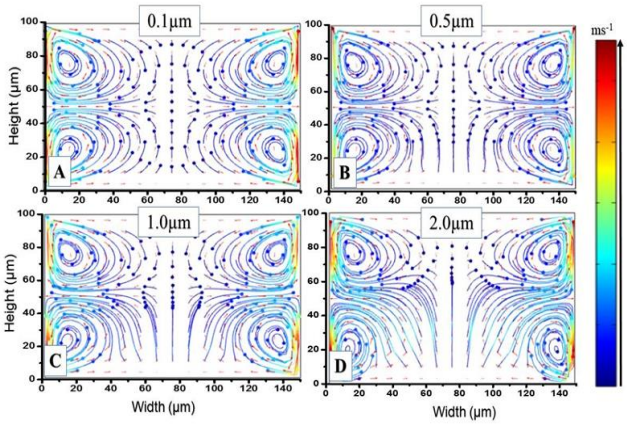

Figure 5. The trajectories (coloured lines) and places (dots) attained via combined electrophoresis and acoustophoresis at t = 5 s for four distinct particle diameters are shown in four panels at frequency 5.0MHz: 0.1 μm, 0.5 μm, 1.0 μm and 2.0 μm are the different sizes.

Figure A features polystyrene particles with a radius of 0.1 μm, where the prevailing force driving particle motion is the acoustic streaming force due to ACP, overshadowing the influence of the repulsion force due to DEP. In addition, the repulsion of polystyrene micro-particles can be seen i.e negative DEP. In Figure A, the repulsive effect appears to be relatively weak. However, for particles with radii of a=0.5 μm, a=1.0 μm, and a=3.0 μm, a discernible repulsion effect becomes evident. It can be inferred from these images that the repulsion phenomenon in polystyrene micro-particles intensifies in proportion to an increase in particle radius. The reason is that as particle radii increasing, they become less polarizable than the surrounding medium, which makes them repel towards low electric fields.

CONCLUSION

We proposed a numerical investigation of DEP and ACP in a single chip platform to investigate the dominant force and its conditions. In this study, we constructed three distinct two-dimensional models with a fixed channel dimensions and varied polystyrene diameter. In the first model, we explored ACP force across various polystyrene particle sizes, finding that particles with a 0.1 μm radius were primarily governed by the streaming force, while those with radii of 1.0 μm and 2.0 μm were influenced mainly by the acoustic radiation force. Subsequently, we examined the behavior of polystyrene particles in response

to dielectrophoresis, revealing negative dielectrophoresis at a frequency of 5 MHz and positive dielectrophoresis at 0.4 MHz. Finally, the third case investigated the combined effects of ACP and DEP, revealing a coexistence of streaming effects and negative dielectrophoresis at a frequency of 5 MHz. Moreover, with increasing polystyrene particle size, it becomes evident that Dielectrophoresis (DEP) effect is superior compared to the influence of the streaming effect from ACP. It is worth noting that the validity of these findings could be substantiated through future experimental validation, potentially paving the way for the practical manipulation of a diverse range of biological particles.

ACKNOWLEDGMENTS

This work is financially supported by Fundamental Research Grant (FRGS) Scheme under the grant number of FRGS/1/2020/STG02/UKM/02/1 from Ministry of Higher Education Malaysia (MOHE).

REFERENCES

[1] Bhatia, S. N., & Ingber, D. E. (2014). Microfluidic organs-on-chips. *Nature biotechnology*, *32*(8), 760-772.

[2] Aiordachioaie Y. Zhang and P. Ozdemir, "Microfluidic DNA amplification—A review," Analytica chimica acta, vol. 638, pp. 115-125, 2009.

[3] Zhang, C., Xu, J., Ma, W., & Zheng, W. (2006). PCR microfluidic devices for DNA amplification. Biotechnology advances, 24(3), 243-284.

[4] D. K. Nasiri, R., Shamloo, A., Ahadian, S., Amirifar, L., Akbari, J., Goudie, M. J., ... & Khademhosseini, A. (2020). Microfluidic-based approaches in targeted cell/particle separation based on physical properties: Fundamentals and applications. Small, 16(29), 2000171.

[5] Fröhlich, J., Hafemann, T. E., & Jain, R. (2022). Phase-resolving direct numerical simulations of particle transport in liquids—From microfluidics to sediment. *GAMM-Mitteilungen*, *45*(2), e202200016.

[6] Fröhlich, J., Hafemann, T. E., & Jain, R. (2022). Phase-resolving direct numerical simulations of particle transport in liquids—From microfluidics to sediment. *GAMM-Mitteilungen*, *45*(2), e202200016.

[7] Cardenas-Benitez, B., Jind, B., Gallo-Villanueva, R. C., Martinez-Chapa, S. O., Lapizco-Encinas, B. H., & Perez-Gonzalez, V. H. (2020). Direct current electrokinetic particle trapping in insulator-based microfluidics: Theory and experiments. *Analytical Chemistry*, *92*(19), 12871-12879.

[8] Zhou, X., Li, Z., Zhang, Z., Zhu, L., & Liu, Q. (2022). A rapid and label-free platform for virus enrichment based on electrostatic microfluidics. *Talanta*, *242*, 122989.

[9] Bhagat, A. A. S., Bow, H., Hou, H. W., Tan, S. J., Han, J., & Lim, C. T. (2010). Microfluidics for cell separation. *Medical & biological engineering & computing*, *48*, 999-1014.

[10] Petersson, F., Åberg, L., Swärd-Nilsson, A. M., & Laurell, T. (2007). Free flow acoustophoresis: microfluidic-based mode of particle and cell separation. *Analytical chemistry*, *79*(14), 5117-5123.

[11] Gascoyne, P. R., & Vykoukal, J. (2002). Particle separation dielectrophoresis. *Electrophoresis*, *23*(13), 1973.

[12] Erdem, N., Yıldızhan, Y., & Elitaş, M. (2017). A numerical approach for dielectrophoretic characterization and separation of human hematopoietic cells. *International Journal of Engineering Research & Technology (IJERT)*, *6*(4), 1079-1082.

[13] Zhang, J., Song, Z., Liu, Q., & Song, Y. (2020). Recent advances in dielectrophoresis-based cell viability assessment. *Electrophoresis*, *41*(10-11), 917-932.

[14] Yildizhan, Y., Erdem, N., Islam, M., Martinez-Duarte, R., & Elitas, M. (2017). Dielectrophoretic separation of live and dead monocytes using 3D carbon-electrodes. *Sensors*, *17*(11), 2691.

[15] Cetin, B., Özer, M. B., & Solmaz, M. E. (2014). Microfluidic bio-particle manipulation for biotechnology. *Biochemical engineering journal*, *92*, 63-82.

[16] Kandemir, M. H., Wagterveld, R. M., Yntema, D. R., & Keesman, K. J. (2019). selective particle Filtering in a Large Acoustophoretic serpentine Channel. *Scientific reports*, *9*(1), 7156.

[17] Friend, J., & Yeo, L. Y. (2011). Microscale acoustofluidics: Microfluidics driven via acoustics and ultrasonics. *Reviews of Modern Physics*, *83*(2), 647.

[18] Hu, Y., Zhong, W., Wan, J. M., & Alfred, C. H. (2013). Ultrasound can modulate neuronal development: impact on neurite growth and cell body morphology. *Ultrasound in medicine & biology*, *39*(5), 915-925.

[19] Hoop, M., Chen, X. Z., Ferrari, A., Mushtaq, F., Ghazaryan, G., Tervoort, T., ... & Pané, S. (2017). Ultrasound-mediated piezoelectric differentiation of neuron-like PC12 cells on PVDF membranes. *Scientific reports*, *7*(1), 4028.

[20] Cetin, B., Özer, M. B., Çağatay, E., & Büyükkocak, S. (2016). An integrated acoustic and dielectrophoretic particle manipulation in a microfluidic device for particle wash and separation fabricated by mechanical machining. *Biomicrofluidics*, *10*(1).

[21] Sun, H., Ren, Y., Hou, L., Tao, Y., Liu, W., Jiang, T., & Jiang, H. (2019). Continuous particle trapping, switching, and sorting utilizing a combination of dielectrophoresis and alternating current electrothermal flow. *Analytical chemistry*, *91*(9), 5729-5738.

[22] Shigemitsu, R., Tagawa, T., & Ozoe, H. (2003). Numerical computation for natural convection of air in a cubic enclosure under combination of magnetizing and gravitational forces. *Numerical Heat Transfer, Part A: Applications*, *43*(5), 449-463.